Journal of the Korean Magnetic Resonance Society **2007**, *11*, 95 - 109

V(IV) Species, Location and Adsorbate Interactions in VH-SAPO-42 Studied by ESR and Electron Spin-Echo Modulation Spectroscopies

Gernho Back,[1*] Jong-Sung Yu,[2] Hyeyoung Lee,[1] Minsik Kim[2] and Yong-Ill Lee[1]

[1]Department of Chemistry, Changwon National University, 9, Sarim-dong, Changwon, Kyungnam 641-773, Korea
[2]Department of Chemistry, BK21 NanoBio Sensor Research Team, Hannam University, 461-6 Jeonmin-dong, Yuseong-gu, Daejeon 305-811, Korea
Received May 15, 2007

Abstract : Vanadium-incorporated aluminophosphate microporous molecular sieve VH-SAPO-42 has been studied by electron spin resonance(ESR) and electron spin-echo modulation (ESEM) spectroscopies to determine the vanadium location and interaction with various adsorbate molecules. The results are interpreted in terms of V(IV) ion location and coordination geometry. As-synthesized VH-SAPO-42 contains only vanadyl species with distorted octahedral or trigonal bipyramidal coordination. Vanadium incorporated into H-SAPO-42 occupied extra-framework site. After calcinations in O_2 and exposure to moisture, only species A is observed with reduced intensities. Species A is identified as a $VO(H_2O)_2^{2+}$ complex coordinated to three framework oxygen atoms bonded to aluminum. When hydrated VH-SAPO-42 is dehydrated at elevated temperature by calcination, species A loses its water ligand and transforms to VO^{2+} ions coordinated to three framework oxygens (species B). Species B reduces its intensities significantly after treatment with O_2 at high temperature, thus suggesting oxidation of V^{4+} to V^{5+}. When dehydrated VH-SAPO-42 makes contact with D_2O at room temperature, the ESR signal of species A is regained. The species is assumed as a $VO(O_f)_3(D_2O)_2$ by considering three framework oxygens. Adsorption of deuterated methanol on dehydrated VH-SAPO-42 results in another new vanadium species D, which is identified as a $VO(CD_3OH)_2$ complex. When deuterated ethylene is adsorbed on dehydrated VH-SAPO-42, another new vanadium species E identified as a $VO(C_2D_4)^{2+}$, is observed. Possible coordination geometries of these various complexes are discussed.
Keywords: SAPO, Vanadium, Molecular Sieve, ESR, ESEM

*To whom correspondence should be addressed. E-mail : ghbaek@changwon.ac.kr

INTRODUCTION

Vanadium-exchanged molecular sieves (e.g., VS-1, VS-2, and VMCM-41, etc) and aluminophosphate molecular sieves (e.g., VAPO-5, and VAPO-11, etc) exhibit interesting catalytic activity in several oxidation and ammoxidation reaction.[1,2] The activity of V^{4+} species is found to depend on the nature and location of the metal ions and on their accessibility and coordination with adsorbate molecules. In general, vanadium species exists as two species; it appears that in the microporous crystalline materials the VO^{2+} species is most probable due to a low framework charge and more positively charged species like V^{4+} cannot be easily stabilized.[3,4]

Several studies have been reported on the characterization of vanadium species in aluminophophate molecular sieves. For characterization of these species different techniques have been used by combining various spectroscopic methods; e.g., electron spin resonance(ESR) ,[5-8] Raman spectroscopy method[9], diffuse reflectance spectroscopy method,[10] and vanadium-51 NMR.[11]

V-incorporated molecular sieves (V-AlMCM-41, VH-SAPO-11, VH-SAPO-34, and VO^{2+}-SAPO-5) can be synthesized using different organic templates and vanadium sources.[4, 21, 26-27] The oxidation state of vanadium in the final product largely depends on the vanadium source used. Vanadium is mostly found as V^{4+} when vanadyl sulfate-containing solution is used as the vanadium source. However, both V^{4+} and V^{5+} are found in V-AlMCM-41 when V_2O_5 is used, which suggests that some V^{5+} is reduced to V^{4+} during gel preparation.[26] Prakash et al. suggested that in VAPO-5 about 10% of the total vanadium is found as isolated V^{4+} and rest is to be VO_x species.[12] On the basis of ^{51}V NMR and diffuse reflectance studies, distorted octahedral or square pyramidal coordination was suggested for V^{5+} in VAPO-5 containing a low vanadium concentration after calcinations and subsequent exposure to moisture.

Silicoaluminophophate-n (SAPO-n) molecular sieves are a new class of microporous crystalline materials comparable to zeolites. A three-dimensional framework is composed of SiO_4, PO_4, and AlO_4 tetrahedrals connected through shared oxygen atoms. This arrangement results in an open structure containing channels and cages of molecular size. The structure of SAPO molecular sieves includes novel structure as well as structure

types analogous to certain zeolites. SAPO-42 is isostructural with zeolite A but shows a much lower cation-exchange capacity.

Studies on adsorbate interactions of vanadium in vanadium-incorporated molecular sieves in general and particularly in VH-SAPO-42 are limited. No systematic effort has been made to identify the various complexes of vanadium with external molecules, notwithstanding the fact that they are of considerable significance in catalysis. Previously, electron spin resonance (ESR) and electron spin-echo modulation (ESEM) spectroscopies have been effectively used to probe various transition metal ions such as V, Mn, Pd, Mo, etc and their coordination geometry with adsorbate molecules in zeolite and aluminophosphate-based molecular sieves.[12-15] While ESR can be used to deduce the local symmetry of the transition metal ions, analysis of the ESEM signals yields the number and coordination distance of associated ligands. In the present paper we describe ESR and ESEM studies on VH-SAPO-42 molecular sieve to obtain information on the nature, location, and adsorbate interactions of vanadium in this material.

EXPERIMENTAL

The synthesis of SAPO-42 was carried out by a modification of the reported methods given in the Union Carbide patent, example 48[16] and in the paper by Zamadics and Kevan[17] using tetramethylammonim hydroxide as the organic template. The quantities, 0.010g of V_2O_5 (Aldrich) and 0.5 g of H-SAPO-42, were mixed in a mortar with pestle for about 30 min. The mixture was pressed in a stainless-steel die to make a pellet of 12 mm diameter and 2.5 mm thickness. The pellet was put in a quartz boat and heated in a furnace at 600 °C in O_2 for 15 h. This calcined sample was cooled slowly to room temperature. Before and after this solid state reaction, the sample was white. The template-free VH-SAPO-42 loses its crystallinity slowly with moisture; the samples were stored under vacuum dessicator.

To examine the influence of dehydration conditions on vanadium agglogation, a hydrated VH-SAPO-42 was first loaded into 3 mm outer diameter and 2 mm inner diameter Suprasil quartz tubes and evacuated at room temperature. Evacuation was

continued by slowly raising the temperature to 300 °C for 3 h where the temperature was maintained. The evacuated samples were heated under 230 Torr of dry oxygen at 300 °C for 4 h, and then evacuated at this temperature for 1 min to remove adsorbed oxygen. Evacuation was continued by slowly raising to 500 °C where the temperature was maintained for 6 h. The sample was then cooled to room temperature to give a dehydrated sample (Note the EPR spectrum in Figure 2c) Finally, the dehydrated sample was heated subsequently in vacuum to 500 °C for about 5 h to give an activated sample. The activated samples were exposed to liquid adsorbates (D_2O and CD_3OH) at their room temperature vapour pressure or to gaseous adsorbates (C_2D_4) as specified in the figure captions. All adsorbates were obtained from Cambridge Isotope Laboratories. The sample tubes were sealed after exposure to adsorbates and were stored in liquid nitrogen.

The V-ion exchange and calcinations of as-synthesized SAPO-42 were examined by the use of a powder X-ray diffraction (XRD) with a Phillips PW 1840 diffractometer. Thermogravimetric analyses were performed by a Dupon 951 thermal analyzer with a heating rate of 10 °C min^{-1}.

ESR spectra were recorded with a modified Varian E-4 spectrometer interfaced to a Tracer Norton TN-1710 signal averager at 77 K. Each spectrum was obtained by multiple scan to achieve a satisfactory signal-to-noise ratio. Each acquired spectrum was transferred from the signal averager to an IBM PC/XT compatible computer for analysis and plotting. The magnetic field was calibrated with a Varian E-500 gauss meter. The microwave frequency was measured at 4.8 K with a Bruker ESP 380 pulsed ESR spectrometer. The pulse echoes were measured by using a 90°-τ-90°-T-90° pulse sequences with $\tau = 0.26 \sim 0.28$ μs, and echo intensity was measured as a function of T. The best-fit simulation for an ESEM spectrum was found by varying the parameters until the sum of the squared residuals between simulated and experimental spectra was minimized. Typical parameters obtained were N to the nearest integer, ±0.01 nm for R, and ±10% for A_{iso}. The theory and simulation of ESEM were described elsewhere.[18-19]

RESULTS

VH-SAPO-42 sample was characterized by powder XRD, and crystallinity and phase purity were confirmed (Fig. 1). The observed XRD patterns match well with the pattern reported for the MFI structure type.[17,20] Practically no loss in crystallinity was observed when an as-synthesized sample was heated at 873K for 15h to remove the organic template. The chemical composition of VH-SAPO-42 was estimated by the characteristic X-ray of specific elements analyzed on a number of crystals. The average chemical compositions of the sample was found to be $(V_{0.01}Al_{0.13}Si_{0.12}P_{0.02})O_2$, which correspond to ~1V in 100unit cells.

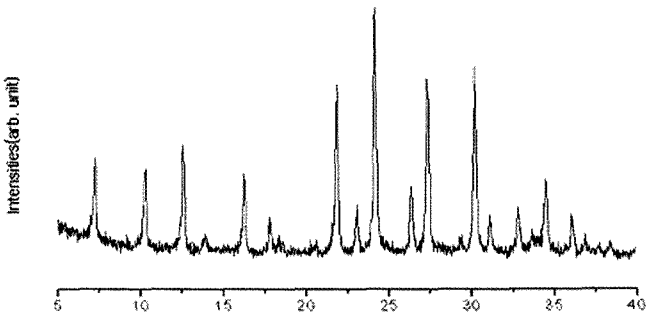

Fig. 1. XRD pattern of as-synthesized SAPO-42

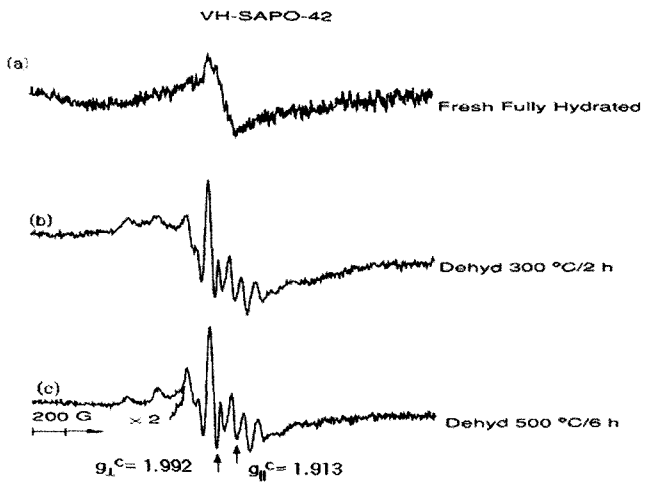

Fig. 2. ESR spectra VH-SAPO-42 recorded at 77 K: (a) fresh, (b) evacuated at 300 °C for 2 h, and (c) evacuated at 500 °C for 6 h.

ESR spectrum of as-synthesized fully-hydrated VH-SAPO-42 was shown in Fig. 2a. The spectrum consists of one axially symmetric signal designated here as species A with hyperfine structure. The ESR parameters were $g_{\|}^{A} = 1.933$ and $A_{\|}^{A} = 184 \times 10^{-4}$ cm^{-1}, and $g_{\perp}^{A} = 1.996$ and $A_{\perp}^{A} = 68.1$ cm^{-1}. Because of overlap with the parallel components, ESR parameters of the perpendicular components, though resolved, were less accurate than the parallel components. These parameters were typical of VO^{2+} with distorted octahedral coordination.[12,20] The spectrum shows hyperfine structure due to interaction of an unpaired $3d^1$ electron with ^{51}V nucleus, that was present in 99.76% abundance with 7/2 nuclear spin. In addition, second-order effect produces asymmetric hyperfine patterns with unequal separation of the lines. The well-resolved hyperfine structure supports a high dispersion of the VO^{2+} ions in SAPO-42. Moreover, no broad back ground signal due to polynuclear oxidized vanadium, which was normally present in samples prepared with high vanadium contents, was observed. Immediately after calcinations in dry oxygen, VH-SAPO-42 does not show any signal suggesting the completely oxidation of VO^{2+} to V^{5+} during calcinations (not shown). A calcined sample was normally exposed to room-temperature humidity before evacuation and dehydration treatments and thus, was hydrated. This calcined, fully-hydrated sample shows weak ESR signal (Fig. 2a). However, the calcined sample after oxidation treatment at 573 K for 4 h and before hydration to RT humidity shows an ESR signal that was weaker than that of a calcined, hydrated sample. Thus, in the calcined materials, most vanadium ions were oxidized to state (V), as can be concluded from the presence of a single weak signal. On the other hand, the ESR spectrum of VH-SAPO-42 after dehydration at 773 K for 5 h for the previously oxidized sample shows only a single axially symmetric signal with hyperfine structure, designated here as species C (Fig. 2c). The ESR parameters were $g_{\|}^{C} = 1.913$ and $A_{\|}^{C} = 180 \times 10^{-4}$ cm^{-1}, and $g_{\perp}^{C} = 1.992$ and $A_{\perp}^{C} = 73.8 \times 10^{-4}$ cm^{-1}. These parameters were significantly different from those of species A. A possible impurities, like e.g., a vanadium (IV) pentoxide was expected to contain dimeric or polymeric vanadyl units which give rise to a broad singlet at room temperature.[17]

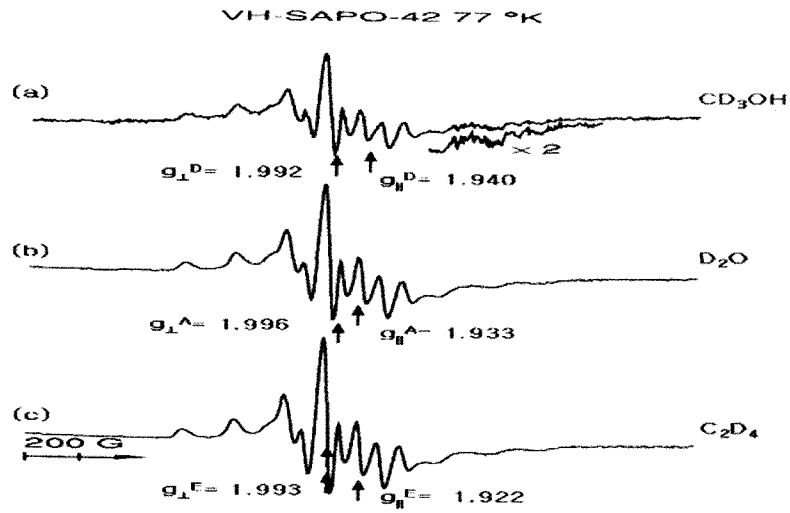

Fig. 3. ESR spectra of VH-SAPO-42 recorded at 77 K: (a) with adsorbed methanol, (b) with adsorbed D_2O, and (c) with adsorbed C_2D_4.

Fig. 3b shows ESR spectrum when D_2O was adsorbed on dehydrated VH-SAPO-42 at room temperature for 20 min. A single vanadium species, whose parameters was identical to that of species A, was observed on adsorption of D_2O on VH-SAPO-42. This results suggest that species A was an aquo-vanadyl complex. The ESR spectrum recorded on VH-SAPO-42 after adsorption of deuterated methanol shows a new vanadium species D characterized by $g_{\|}^{D} = 1.933$ and $A_{\|}^{D} = 181 \times 10^{-4}$ cm^{-1}, and $g_{\perp}^{D} = 1.992$ and $A_{\perp}^{D} = 70.4 \times 10^{-4}$ cm^{-1} (Fig. 3a). Also when deuterated ethylene was adsorbed on dehydrated VH-SAPO-42, a new species E with ESR parameters $g_{\|}^{E} = 1.922$ and $A_{\|}^{E} = 185 \times 10^{-4}$ cm^{-1}, and $g_{\perp}^{E} = 1.993$, and $A_{\perp}^{E} = 71.0 \times 10^{-4}$ cm^{-1} was observed. The ESR parameters and possible assignments of various vanadium species observed in VH-SAPO-42 molecular sieve is summarized in Table 1.

Table 1. ESR Parameters and Assignments of Various Vanadium Species Observed in VH-SAPO-42 Molecular Sieve.

Treatment	Species	Assignments	$g_{\parallel}$	$A_{\parallel}$ [a]	$g_{\perp}$	$A_{\perp}$ [a]
Calcined- hydrated	A	VO^{2+}-$(H_2O)_2$				
Oxidized	B	V^{5+}				
Dehydrated	C	VO^{2+}	1.913	180	1.992	73.8
CD_3OH	D	VO^{2+}-$(CD_3OH)_2$	1.940	181	1.992	70.4
D_2O	A	VO^{2+}-$(D_2O)_2$	1.933	184	1.996	68.1
C_2D_4	E	VO^{2+}-(C_2D_4)	1.922	185	1.993	71.0

[a] x 10^{-4} cm^{-1}

Three-pulse ^{2}D ESEM spectra were recorded at around a magnetic field of 3400 G and at a microwave frequency of 9.854 GHz for various VO^{2+} species. The echo signal was maximum around this field. The delay between the first and second pulses (τ) was selected so as to minimize modulation from other magnetic nuclei present in the system. Fig. 4 was given the experimental and simulated ^{2}D ESEM spectrum of VH-SAPO-42 after adsorption of deuterated methanol. The interpulse time τ was selected as 0.26 μs. Simulation of the spectrum gives six deuteriums at 4.6 Å. These values are consistent with two CD_3OH molecules directly coordinating with VO^{2+} ions in species D. Fig. 5 shows the experimental and simulated ^{2}D ESEM spectrum of VH-SAPO-42 after deuterated ethylene adsorption. The magnetic field and τ values were the same as for adsorbed CD_3OH. The spectrum was simulated with two deuteriums at 4.2 Å and another two deuteriums at 5.5 Å. These parameters can be rationalized in terms of one ethylene coordinating with V^{4+} ions in species E.

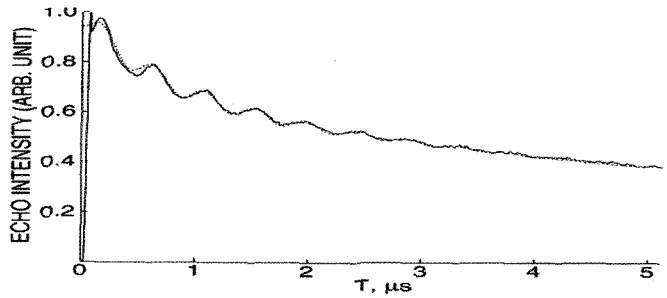

Fig. 4. Experimental(-) and simulated (---) three-pulse ESEM signal at 4 K of VH-SAPO-42 with adsorbed CD_3OH(N= 6.0, R=0.46 nm, A= 0.07 MHz).

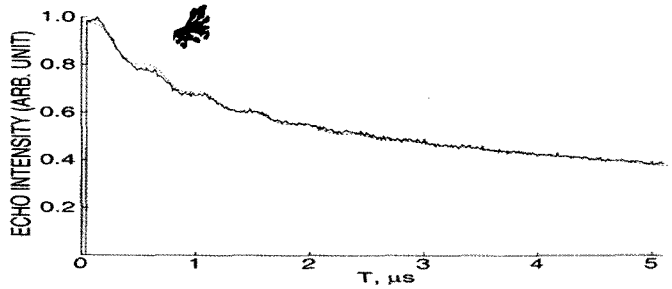

Fig. 5. Experimental(-) and simulated (---) three-pulse ESEM signal at 4 K of VH-SAPO-42 with adsorbed C_2D_4. (N=2, R=0.42 nm, A=0.08, N'=2, R'=0.55 nm, A'=0.082)

DISCUSSIONS

Structure The framework of SAPO-42 is similar to that of zeolite A. The skeleton of this molecular sieve is built from truncated octahedra linked together through double four-membered rings. Each octahedron sits on the vertices of a cube. The connection of the octahedra results in a central cavity referred to as the α-cage. This central cavity is connected to six similar cavities by an eight-membered ring with an opening diameter of 0.42 nm. The truncated octahedra form a set of smaller cavities denoted as β-cages. Entrance into β-cage is achieved through a six-membered ring which has an opening diameter of about 0.20 nm. Fig. 6 illustrates approximately half of the unit cell of SAPO-42.

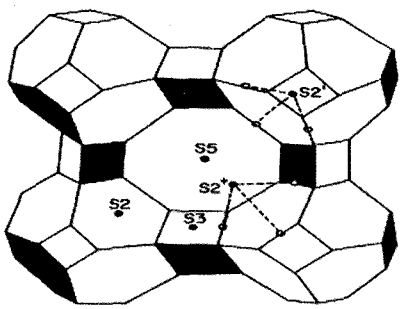

Fig. 6. Crystal structure of SAPO-42 molecular sieve showing possible cation positions.

Probable cation positions can be made from those sites found in its structural analog, zeolite A as proposed by Maggie et al.[17] These locations are indicated in Fig. 6. Site S2 is at the center of the hexagonal faces, and sites S2′ and S2* are shifted away from the hexagonal faces into the β-cage and α-cage, respectively, along a 3-fold perpendicular to the hexagonal window, and site S3 is near the square faces located in the α-cage.

In the various cationic forms of zeolite A, the hydrated Cu(II) complex is reported to be located in site S2′ based on the aid of Cs^+ modulation and a knowledge of the Cs^+ location within molecular lattice from the single crystal X-ray diffraction studies.[17] The hydrated Cu(II) complex in hydrated Rb-SAPO-42 is also reported to be located in site S2′. This conclusion is drawn with the aid of the depth for the Al-modulation pattern.[17]

Dehydration Process The ESR parameters of VO^{2+} in VH-SAPO-42 adsorbed with D_2O are comparable to corresponding values in VH-SAPO-11 where VO^{2+} has octahedral coordination with tetragonal distorsion,[21] and to a pentacoordinate Cu(II) species of CuNa-SAPO-42.[17] A pentacoordinated Cu(II) complex, where the Cu(II) ion is coordinate to two water ligands and three framework oxygens, is most likely based on the result of ESEM. A configuration of this type could exist at site S2* in the α-cage or site S2′ in the β-cage. The Vanadium(IV) normally enters into compound as oxovanadium (IV) commonly called "vanadyl" entity VO^{2+} and exhibits paramagnetic resonance absorption due to a single unpaired electron. The electronic state of VO^{2+} ion is normally depend on the $3d^1$ electron of vanadium and therefore, the levels of VO^{2+} are similar to those of the V^{4+} ion. When a vanadyl ion is incorporated into a crystal lattice by coordination with other ligands, it is subject to a crystal field due to the surrounding environment. The most common coordination of vanadium is octahedral or square pyramidal often with tetragonal distorsion.[17] The electronic structure of the $VO(H_2O)_5^{2+}$ complex, where vanadium ion is in an octahedral coordination with oxygen ligands having tetragonal distortion, is observed in a number of compounds such as $VOSO_4 \cdot 5H_2O$.[22] On the basis of a LCAO-MO model, it has been shown that the unpaired electron occupies a nonbonding b_2 type of vanadium orbital ($3d_{xy}$) and that the lowest state becomes an orbital singlet. Later, this model is successfully extended to a large number of vanadium compounds with various crystalline symmetries and also to compounds where vanadium ions have

different coordination number or ligands.[23,24] The ESR spectra of VO^{2+} are complicated by the high number of hyperfine levels generated due to magnetic interaction with the vanadium nucleus and by second effects that tend to produce an asymmetric hyperfine structure with unequal separation of the various lines.

ESR The thermally reduced VH-SAPO-42 samples give similar ESR signals at room temperature. The example is explained in Figure 2c. The spectrum can be characterized by two axially symmetric sets for eight lines originating from vanadyl VO^{2+} species coupled to its own nuclear spin (^{51}V, I_N = 7/2, natural abundance 99.8%). The well-resolved hyperfine structure supports a high dispersion of the VO^{2+} ions in H-SAPO-42.

The low intensity of species A observed in calcined, hydrated VH-SAPO-42 is indicative of oxidation of some of the V^{4+} ion to V^{5+} ion during calcinations in dry O_2. Upon evacuation of calcined, hydrated VH-SAPO-42, the ESR spectrum changes significantly, and finally, after dehydration at 773 K a new species C is observed. Species C is probably VO^{2+} with no water or hydroxyl ligands and coordinated with only framework oxygens. The observation that species A transforms to species C by evacuation at room temperature or at elevated temperature and the species C returns to species A after adsorption to D_2O, is strong indication of the hydrated nature of species A. Although the ESR parameters of some these species are characteristic of the vanadyl ion, the exact nature of the vanadium species is unclear, requiring more quantitative information for the unambiguous assignment of coordination geometry.

Adsorption Adsorption of CD_3OH on dehydrated VH-SAPO-42 generates a new species D with ESR parameters different from those of species C. ^2D ESEM parameters of six deuteriums interacting at 4.6 Å are consistent with that of two ethanol molecules coordinating to the V^{4+} ion. This suggests that the immediate coordination sphere of V involves O ligands. The relatively large distance between V^{4+} and ^2D nuclei suggests a weak interaction for ethanol. A distorted octahedral symmetry for this complex is most likely. Few compounds have been reported in which the coordination of vanadium is type of $(VO)(O_f)_3(CD_3OH)_2$. Vanadium in VAPO-5 has been reported to have square piramidal

coordination environments for the VO^{2+} ions.[12] The ESR parameters of this compounds are comparable to the values observed for species D.

With adsorbed C_2D_4, VH-SAPO-42 shows a new vanadium species E. The yellow color of samples activated at 773 K completely disappeared, and the sample become colorless, indicating a drastic change in the ligand field around V^{4+} ion either through rearrangement of its ligand or by replacement of one or more of the ligand. The color change resulted in the formation of a new spectrum with reversed g value ($g_\perp > g_\parallel$). On adsorption of ethylene for activated sample above 770 K with cupric ion in impregnated silica gel, Narayana et al. suggested that ethylene distorts the $Cu\text{-}O_4$ tetrahedral to form a distorted square-piramidal or trigonal-bipiramidal complex with one of $Cu\text{-}O_1$ bond becomes apical and the shorter than the other three Cu-O bonds.[28] ^2D ESEM parameters of two deuterium at 4.2 Å and two deuterium at 5.5 Å are consistent with one ethylene molecule coordinating with V^{4+}. A possible geometry for this complex is one in which the vanadyl ion has weak σ-bond coordination with a CH_2 group of ethylene molecule to form a distorted tetrahedral complex. A similar bonding behavior is suggested for a Ni(I)-$(C_2D_4)_1$ complex observed after adsorption of ethylene in NiAPSO-11, a medium-pore molecular sieve.[25] On the basis of the ESR and ^2D ESEM results, possible coordination geometries of the vanadium species observed in VH-SAPO-42 after adsorption of various adsorbates are given in Fig. 7. It should be noted that unlike Ni in NiAPSO-5, VH-SAPO-42 contains the VO^{2+} ion, which includes vanadyl oxygens, incorporated into extra-framework. Thus the presence of the vanadyl oxygen and its orientation inside the channel are factors that may influence the formation and the nature of metal-adsorbate complexes in VH-SAPO-42 and other vanadium-incorporated molecular sieves.

CONCLUSIONS

Electron spin-echo modulation spectroscopy, when coupled with electron spin resonance spectroscopy, has been showed to be very effective for obtaining information about the nature and location of vanadium in VH-SAPO-42 and also its coordination behavior toward various adsorbates. As-synthesized VH-SAPO-42 contains one VO^{2+}

species A with distorted octahedral symmetry. Species A is considered as a $VO(H_2O)_2^{2+}$ complex coordinated to additional three framework oxygen atoms. During calcinations, part of V^{4+} ions are oxidized to V^{5+}. VH-SAPO-42 after dehydration at elevated temperature shows a new vanadium species C, which is suggested to be VO^{2+} ion with no water or hydroxyl ligands. Adsorption of D_2O on dehydrated VH-SAPO-42 regenerates species A and is assumed as $VO(D_2O)_2^{2+}$ with vanadium coordination of the type $VO(O_2)(O_f)_3$ where O_f is a framework oxygen. Adsorption of deuterated methanol on dehydrated VH-SAPO-42 generates another new vanadium species D identified as $VO(CD_3OH)_2$. When deuterated ethylene is adsorbed on dehydrated VH-SAPO-42, a new vanadium species E identified as $VO(C_2D_4)^{2+}$, with weak σ-bonding is observed.

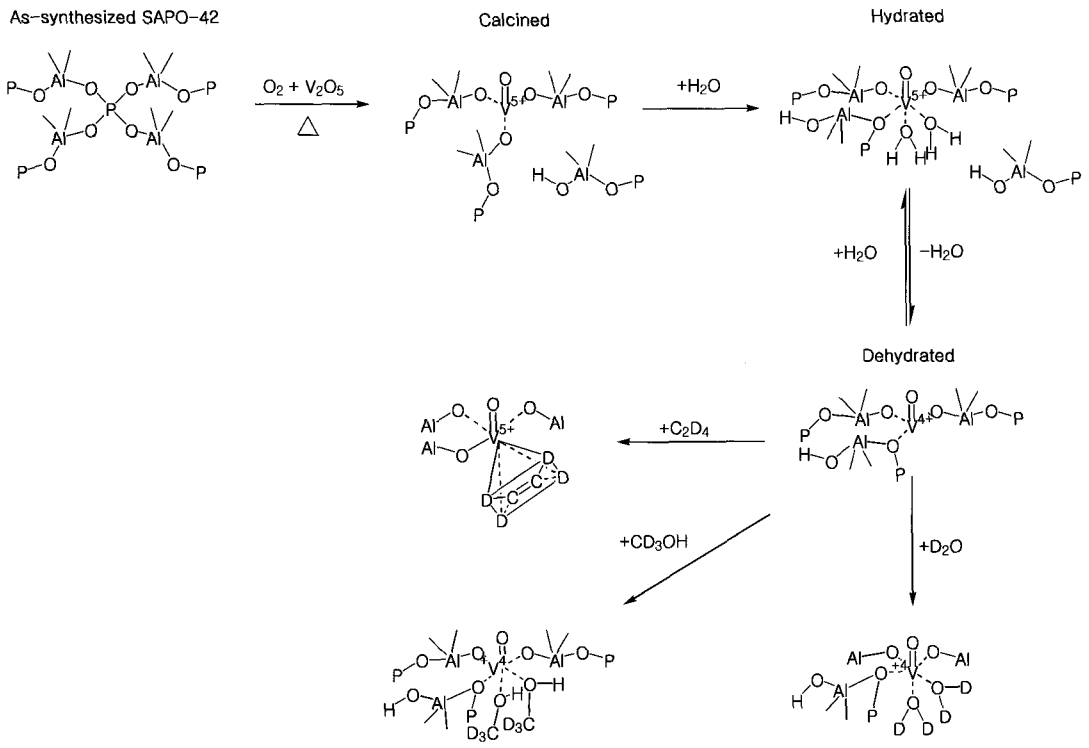

Fig. 7. Proposed model structures for various vanadium-adsorbate complexes in VH-SAPO-42.

Acknowledgements

This research financially was supported by the Changwon National University in 2007. JSYu thanks Hannam University for financial support.

REFERENCES

1. G. Bellusi, and M. S. Rigutto, "Advanced Zeolite Science and Application" J. C. Jansen, M. Stoker, H. G. Karge, and J. Weitkamp, Eds., "Studies in Surface Science and Catalysis 85",Elsevior, Amsteldam, 177-213 (19945)
2. A. Miyamoto, D. Medhanavayn, and I. Inui, *Appl. Catal.* **28**, 89 (1986).
3, E. M. Flanigen, B. M. Lok, R. L. Patton and S. T. Wilson, *Pure Appl. Chem*, **58**, 1351 (1986).
4. G. Back, Y.-S. Cho, Y. Kim and L. Kevan, *J. Kor. Mag. Res. Soc.* **5**(2) 73(2001).
5. T. Ichigawa and L. Kevan, *J. Am. Chem. Soc.* **105**, 402 (1983).
6. X. Chen and L. Kevan, *J. Am. Chem. Soc*, **113**, 2861 (1991).
7. G. Bruet, X. Chen, C. W. Lee and L. Kevan, *J. Am. Chem. Soc.* **114**, 3720 (1992).
8. M. Hartmann, A. Azuma, and L. Kevan, *J. Phys. Chem.* **99**, 10988 (1995).
9. Z. Luan, Paul A. Meloni, R. S. Czernuszewicz and L. Kevan, *J. Phys. Chem. B* **101**, 9046 (1997).
10. S. Dzwigaj, M. Matsuoka, R. Frack, M. Anpo and M. Che, *J. Phys. Chem.* **102**, 6309 (1998).
11. N. Das, H. Eckert, H. Hu, I. E. Wachs, J. F. Walzer and F. J. Feher, *J. Phys. Chem.* **97**, 8240 (1993).
12. A. M. Prakash and L. Kevan, *J. Phys. Chem. B* **103**, 2214 (1999).
13. G. Back, Y. Kim, Y.-Y. Cho, Y.-I Lee and C. W. Lee, *J. Kor. Mag. Res. Soc.* **6**(1), 20 (2002).
14. G.-H. Back, J.-S. Yu, V. Kurshev and L. Kevan, *J. Chem. Soc. Faraday Trans.* **90**(15), 2283 (1994).
15. G. Back, C. Jang, C. Ru, Y. H. Cho, H. So and L. Kevan, *J. Kor. Chem. Soc.* **46**(1) 26 (2002).

16. B. M. Lok, C. A. Messina, R. L. Patton, R. T. Gajek, T. R. Cannon and E. M. Flanigen, US Patent 4440871 (1984).
17. M. Zamadics and L. Kevan, *J. Phys. Chem.* **96**, 1042 (1992).
18. L. Kevan, In *Time Domain Electron Spin Resonance*; L. Kevan and R. N. Schwartz, Eds.,; Wiley: New York, 1979; Chap 8.
19. S. A. Dikanov, A. A. Shubin, and V. N. Parmon, *J. Mag. Res.* **42**, 474 (1981).
20. R. von Ballmoos and J. B. Higgins, *Zeolites* **10**, 386 (1990).
21. G. Back, S.-C. Baek, S.-G. Park and C.W. Lee, *J. Kor. Mag. Res. Soc.* **9**(1), 1 (2005).
22. Ballhausen, C. J and H. B. Gray, *Inorg. Chem.* **1**, 111 (1962).
23. Hecht, H. G. and Johnson T. S. *J. Chem. Phys.* **46**, 23 (1967).
24. Kevelson, D. and Lee, S.-K. *J. Chem. Phys.* **41**, 1896 (1964).
25. N. Azuma, C.W. Lee and L. Kevan, *J. Phys. Chem.*, **98**, 1221 (1994).
26. G. Back, J.-S. Yu, H. Lee, and Y.-I. Lee. *J. Kor. Mag. Res. Soc.* **20**(2), 141 (2006).
27. G. Back, S.-G. Park, and C.W. Lee, *J. Kor. Mag. Res. Soc.* **9**(1), 138 (2005).
28. M. Narayana, R.Y. Zhan, and Larry Kevan, *J. Phys. Chem.* **88**, 3990 (1984).